Chromatin fine structure profiles for a developmentally regulated gene: reorganization of the lysozyme locus before trans-activator binding and gene expression

Joanna Kontaraki,[1] Hsiu-Hua Chen,[2] Arthur Riggs,[2] and Constanze Bonifer[1,3]

[1]University of Leeds, Molecular Medicine Unit, St. James's University Hospital, Leeds LS9 7TF, UK; [2]Department of Biology, Beckman Institute of City of Hope, Duarte, California 91010 USA

The chicken lysozyme locus is activated in a stepwise fashion during myeloid differentiation. We have used this locus as a model to study at high resolution changes in chromatin structure both in chicken cell lines representing various stages of macrophage differentiation and in primary cells from transgenic mice. In this study we have addressed the question of whether chromatin rearrangements can be detected in myeloid precursor cells at a stage well before overt transcription of the lysozyme gene begins. In addition to restriction enzyme accessibility assays and DMS footprinting, we have applied new, very sensitive techniques to assay for chromatin changes. Particularly informative was UV photofootprinting, using terminal transferase-dependent PCR and nonradioactive detection. We find that the basic chromatin structure in lysozyme nonexpressing hematopoietic precursor cells is highly similar to the pattern found in fully differentiated lysozyme-expressing cells. In addition, we find that only in nonexpressing cells are dimethylsulfate footprints and UV photofootprints affected by trichostatin, an inhibitor of histone deacetylation. These results are interpreted to mean that most chromatin pattern formation is complete before the binding of end-stage trans-activators, supporting the notion that heritable chromatin structure is central to the stable epigenetic programs that guide development.

Received March 30, 2000; revised version accepted June 21, 2000.

[*Key Words*: Chicken lysozyme gene; cell differentiation; transcriptional regulation; chromatin; epigenetics]

The establishment and the heritable maintenance of specific epigenetic states leading to differential gene expression are crucial to development and are the underlying cause for the progressive restriction of the genomic potential during ontogeny (for review, see Kikyo and Wolffe 2000). However, the elucidation of the molecular details of cell differentiation at the level of chromatin structure is still in its infancy. This is mostly because of the difficult nature of the experiments involved and the requirement for studies of chromatin structure-function relationships at one specific gene locus in pure populations of different cell types.

Higher order chromatin structure involving specific multiprotein complexes represents an important level of control in the tissue-specific activation and repression of eukaryotic genes and to a large degree determines the specific epigenetic state of a gene locus. A large number of studies examining chromatin at low resolution [e.g., DNaseI hypersensitive site (DHS) mapping] have linked a specific developmental chromatin structure to differential activities of cis-regulatory elements (Gross and Garrard 1988). The analysis of protein–DNA interactions at single-nucleotide resolution level in vivo has demonstrated that, depending on the developmental stage, different combinations of transcription factors can occupy the same cis-regulatory element (Gualdi et al. 1996; Roque et al. 1996; Shaffer et al. 1997). These experiments suggest that the transcriptional activation of a gene locus is achieved by the cooperation of different cis-regulatory elements that, in turn, assemble transcription factors in a sequential, developmentally controlled fashion. However, very little is known about the influence of the chromatin architecture underlying this process.

The hematopoietic system is well suited for chromatin structure–function studies both because, under the influence of specific cytokines, cell differentiation can be followed in culture and because a large number of different cell lines are available that represent various

[3]**Corresponding author.**
E-MAIL c.bonifer@leeds.ac.uk; FAX 44-113-2444475.

stages of cell differentiation. We have used the chicken lysozyme locus, which is active in myeloid cells, as a model to analyze epigenetic changes in cells representing various macrophage differentiation states, ranging from the multipotent progenitor cell not yet expressing the gene to the terminally differentiated cell type expressing the gene at maximum level. The cis-regulatory elements of the lysozyme locus are well characterized. Three enhancers, located 6.1 kb, 3.9 kb, and 2.7 kb upstream of the transcriptional start site, a silencer element located at –2.4 kb as well as a complex promoter have been identified (for review, see Bonifer et al. 1997) All active cis-regulatory elements colocalize with chromatin DHSs (Fritton et al. 1984, 1987; Huber et al. 1995). The individual enhancer elements of the lysozyme locus can be categorized into early or late enhancers according to their developmental activation profile. The early enhancers at –6.1 kb and –3.9 kb and the promoter become DNaseI hypersensitive at the myeloblast stage when the gene is transcriptionally activated, albeit at a low level. The DHS at the silencer element is still present. The DHS at the late –2.7 kb enhancer appears only later in differentiation at the monocyte/promacrophage stage. Simultaneously, the –2.4 kb silencer DHS disappears (Huber et al. 1995). Studies in which we used micrococcal nuclease (MNase) to probe for positioned nucleosomes in the complete 5′-regulatory region of the lysozyme locus revealed that each cis-regulatory element shows a unique structural organization with the transcription factor binding sites specifically arranged with respect to nucleosomes (Huber et al. 1996). Nucleosomes are reorganized in an element-specific fashion during macrophage differentiation.

At the resolution level of Southern blots, the chromatin structure of the chicken lysozyme locus in transgenic mice is identical to that in chicken cells, and the same type of chromatin rearrangements are observed after gene locus activation (Huber et al. 1994, 1996). We have purified early macrophage precursor cells from transgenic mice carrying wild-type and deletion constructs and subjected these cells to in vitro differentiation under macrophage growth–promoting conditions (Jägle et al. 1997). We could show that developing mouse macrophage cells upregulate transcription of the chicken lysozyme transgene at the same developmental stage as chicken macrophages (Myeloblasts/GM-CFCs). The early enhancers and the promoter are sufficient to activate the chicken lysozyme gene at the correct, early developmental stage, where a deletion of the early –6.1-kb enhancer leads to a delay in gene activation. In addition, the different enhancers possess an intrinsic difference in their chromatin reorganizing capacity. The analysis of a construct carrying the complete lysozyme locus with an internal deletion of the promoter in transgenic mice (Huber et al. 1997) revealed that the formation of a DHS at the –2.4 kb silencer element and the –2.7 kb enhancer element was unaffected. In contrast, DHS formation and chromatin remodeling at the early –6.1-kb and –3.9-kb enhancers were totally abolished.

Taken together, these studies indicate that the activation of the lysozyme locus occurs as a cooperative process in which the early enhancers have to interact with the promoter in order to form a stable enhancer–promoter complex indicated by a DHS in chromatin. At present, the molecular details of this enhancer-promoter interaction as well as the factors involved in this process are unknown. To this end, we have taken our analysis of the chromatin structural changes taking place during cell differentiation one step further and here report a study in which we have examined chromatin fine structure and transcription factor occupancy at the lysozyme early enhancers and the promoter at the nucleotide resolution level during macrophage differentiation. In particular, we examined whether any epigenetic differences exist between cells destined to become macrophages and cells belonging to a different lineage within the hematopoeitic hierarchy. Using a novel quantitative UV photofootprinting technique, we gathered detailed information about the chromatin fine structure at the individual cis-regulatory elements. We have been able to determine that a specific chromatin pattern is already established in multipotent precursor cells that show no chromatin reorganization at low level resolution, do not show binding of transcription factors crucial for lysozyme gene expression over enhancer and promoter regions, and do not express the gene. Our results indicate a developmentally controlled maturation of chromatin that is likely to be independent of the end-state transcription factors controlling gene expression in differentiated cells.

Results

Activation of the chicken lysozyme locus leads to a differential restriction enzyme accessibility of the 5′ regulatory region

Retrovirally transformed cell lines have been used to analyze the structural reorganization of the chicken lysozyme gene locus during macrophage differentiation (Huber et al. 1995, 1996). Several transformed cell lines have been generated, representing various differentiation stages within the myeloid lineage (Metz and Graf 1991; Graf et al. 1992). The cell line HD50 MEP resembles multipotent progenitor cells that can be induced to differentiate into eosinophils or myeloblasts. Differentiation of MEP cells generated the myeloblast cell line HD50 myl and eosinophil-like cells (1A1; Kulessa et al. 1995). We recently discovered that the lysozyme gene that was originally thought to be expressed only in macrophages is also expressed in the eosinophil-like cells as well as in granulocytes from transgenic mice (C. Bonifer, unpubl.). The cell line HD37 resembles erythroblasts. The cell line HD11 (Beug et al. 1979) corresponds to monocytic cells, which can be further stimulated and differentiated by treatment with bacterial lipopolysaccharide (LPS; Huber et al. 1995). The position that these cell lines occupy within the myeloid hierarchy as well as their expression levels from the chicken lysozyme locus are schematically depicted in Figure 2A (see below).

In previous experiments (Huber et al. 1995, 1996;

Kruger et al. 1999), we have gathered extensive information about long-range chromatin rearrangements over the entire 5′ regulatory region of the lysozyme locus in the cell lines described in Figure 2 as well as in transgenic mice. This includes the mapping of DNaseI hypersensitive sites and low-resolution MNase mapping. Here we employed an in vivo restriction enzyme assay to determine whether the recognition sequences were covered by a nucleosome or another factor complex (Straka and Hörz 1991). In the lysozyme locus, recognition sequences for the restriction enzyme *Hin*fI are present in basically every cis-regulatory region. Figure 2B–2D indicates the result of a restriction enzyme accessibility assay determining *Hin*fI accessibility in the chromatin of most of the 5′ regulatory region of the lysozyme locus (schematically summarized in Fig. 1). In most cases, *Hin*fI accessibility coincides with the position of linker regions as mapped by MNase digestion for both lysozyme-expressing and nonexpressing cells. The presence of a DHS did not always lead to an increase in *Hin*fI accessibility as exemplified by the –2.7-kb enhancer/–2.4-kb silencer region (Fig. 2D). Here, positioned nucleosomes cover both elements in lysozyme nonexpressing cells with a DHS over the –2.4-kb silencer region. Activation of the –2.7-kb enhancer in lysozyme-expressing cells leads to DHS formation accompanied by a remodeling of nucleosomes in this area and a subsequent loss of *Hin*fI accessibility. Conversely, in the promoter region, nucleosome remodeling and DHS formation leads to *Hin*fI accessibility (Fig. 2C). In summary, lysozyme-expressing cells show major changes in general chromatin structure over the cis-regulatory elements. In contrast, at the resolution provided by Southern blots, the *Hin*fI accessibility pattern is indistinguishable between the two lysozyme nonexpressing cells analyzed (HD50 MEP and HD37), confirming previous experiments comparing the chromatin structure of a number of different cell types (Fritton et al. 1987; Sippel et al. 1987; Huber et al. 1995, 1996).

UV photofootprinting reveals the formation of an active chromatin pattern in precursor cells before the binding of enhancer and promoter factors

Several previous low-resolution mapping studies did not detect any difference in chromatin structure between erythroid lineage cells such as HD37 and myeloid precursor cells such as HD50 MEP (Huber et al. 1995, 1996). Nevertheless, we wanted to see if UV photofootprinting would be more sensitive and reveal differences in chromatin fine structure (Becker and Wang 1984). The rationale for trying this approach was that in vitro experiments have shown that the pattern of UV adduct formation is affected by even subtle distortions of DNA structure. UV light generates photodimers between adjacent bases, mostly cyclobutane pyrimidine dimers and (six to four) photoproducts. All structural changes that bend DNA toward the major groove enhance, and all

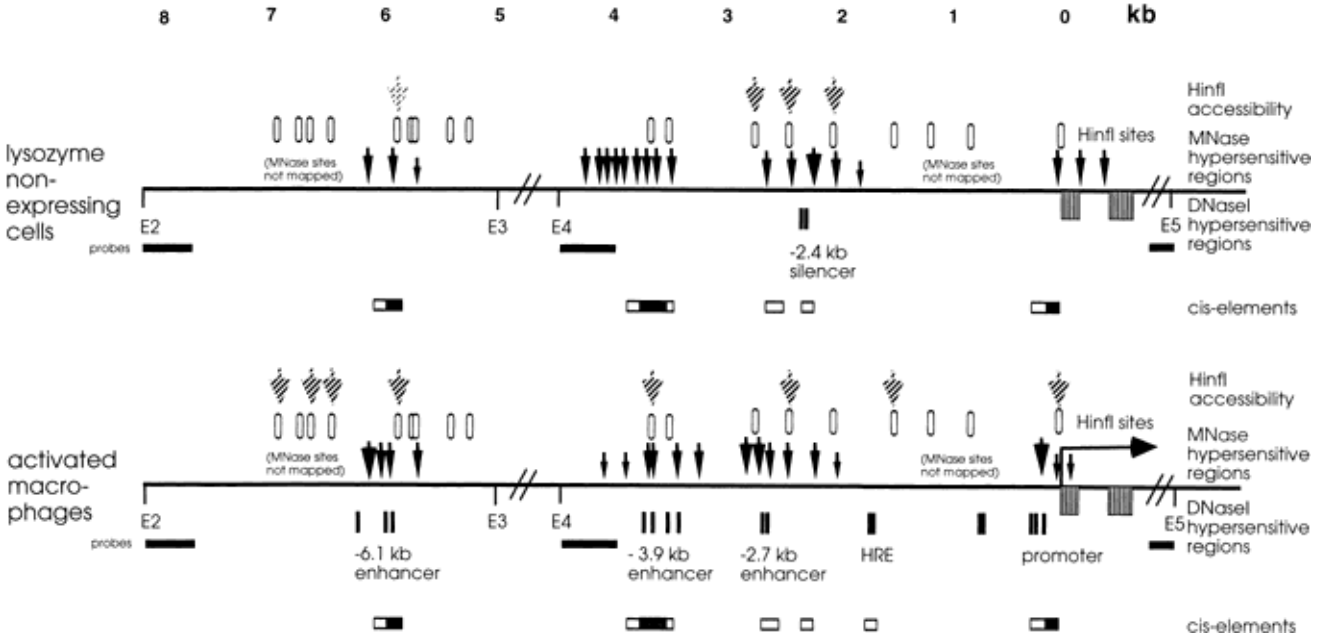

Figure 1. Chromatin features of the 5′ regulatory region of chicken lysozyme locus at low-level resolution. The figure depicts MNase cleavage sites (black vertical arrows), DNaseI hypersensitive sites (black vertical bars), and accessible *Hin*f sites (striped arrows representing accessible sites over gray ovals indicating the position of *Hin*fI sites) in lysozyme nonexpressing cells (upper panel) or activated macrophages expressing the lysozyme gene at maximal level (lower panel). The position of cis-regulatory elements are indicated as white boxes; the regions analyzed by in vivo footprinting are depicted as dark insert. The transcriptional start site is indicated by a horizontal arrow. Exons are depicted as vertically striped boxes. The probes used for restriction enzyme accessibility assays are drawn as black horizontal bars. *Eco*RI fragments (E2–E3; E4–E5) are indicated.

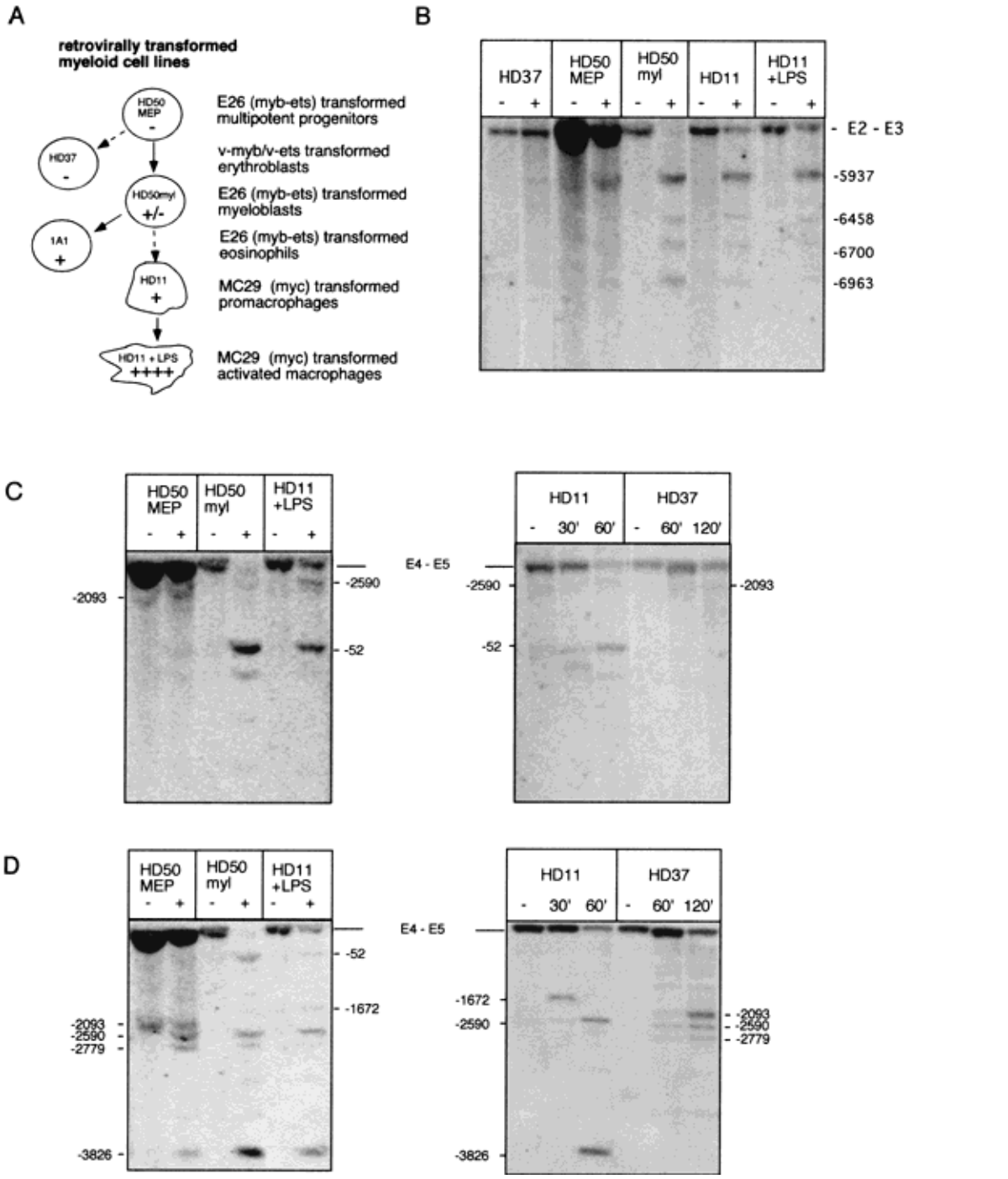

Figure 2. *Hin*fI accessibility of the 5′ regulatory region of chicken lysozyme locus. (*A*) Transformed cell lines analyzed in this study and their position in the hematopoietic hierarchy; their lysozyme expression level is indicated as (+) or (–). The arrows indicate the differentiation direction: solid arrows connect cell lines derived from MEP cells and hatched arrows connect independently derived cell lines. (*B*) Hybridization with an upstream *Hin*dIII probe (–8090––7802 bp). Accessible *Hin*fI sites on restriction fragment E2–E3 including the –6.1-kb enhancer in the cell lines are indicated. (*C*) Hybridization with a 0.8-kb *Hin*dIII/*Xba*I fragment spanning part of intron 1 and exon 2. Accessible *Hin*fI sites on fragment E4–E5 are indicated. (*D*) Hybridization with a *Hin*dIII–*Pvu*II fragment representing the region from –4332 to –3848 bp. Accessible *Hin*fI sites on fragment E4–E5 are indicated. The numbers represent the positions of the accessible sites with respect to the transcription start site. The right panels in (*C*) and (*D*) represent cells incubated for 30 and 60 min, respectively; in the left panel, cells were incubated for 1 hr with the restriction enzyme. MEP lanes contain about five times as much DNA in order to emphasize certain nuclease sensitive sites.

changes which bend DNA away from the major groove reduce, the frequency of UV dimer formation (for review, see Becker and Grossmann 1993). Consequently, the pattern of UV adduct formation is affected by the slight distortions caused by DNA being wrapped around nucleosomes. A 10.3-bp periodicity in photoreactivity is seen, similar to the periodicity seen using DNaseI (Gale et al. 1987). The binding of many transcription factors also increases or decreases dimer formation (Pfeifer et al. 1992). Another advantage of UV photofootprinting is that the treatment is truly in vivo. Live cells are irradiated just before DNA extraction; thus, perturbation of chromatin structure is minimal.

We applied the UV footprinting technique to examine the chromatin fine structure of cis-regulatory elements at the lysozyme locus in the various cell types. In order to visualize all types of UV-generated lesions, to avoid the need for hard-to-obtain enzymes and to achieve the sensitivity needed to analyze vertebrate cells, we have used a modification of the recently developed terminal transferase-dependent PCR (TDPCR) method (Komura and Riggs 1998; Pfeifer et al. 1999), which is based on the fact that primer extension by DNA polymerases is blocked by the presence of DNA lesions such as UV dimers. Another improvement is that we use 5′ fluorescent dye labeling with separation and detection of the PCR-generated DNA fragments by use of a Li-Cor DNA sequencing instrument. This instrument gives well-separated, symmetrical bands over >300 nt and detects fluorescence emission in the near-infrared, which leads to sensitivity compatible to the use of ^{32}P; moreover, the background is constant and very low, leading to accurate quantification.

Figure 3 shows the UV footprinting pattern of the upper strand of the lysozyme promoter in the different cell lines. Previous in vitro and in vivo footprinting experiments in HD11 cells have demonstrated a number of ubiquitous and macrophage-specific protein–DNA interactions in the promoter region between –50 bp and –200 bp (Altschmied et al. 1989; Dölle and Strätling 1990), as indicated in the figure. A number of obvious and subtle differences in the adduct patterns relative to genomic DNA were observed by eye. In addition to those changes in UV dimer formation that cover the known transcription-factor binding sites, there are additional changes specific for lysozyme-expressing cells. Importantly, though, it is also apparent that there are more similarities between lysozyme expressing (HD11) and multipotent nonexpressing precursor cells (HD50 MEP) than between these cells and the erythroblast cell line HD37.

To improve the comparison, we quantified the fluorescence of each band and calculated signal intensities at each nucleotide position for each of the different cell types and genomic DNA (Fig. 4). Figure 4D shows the ratio at each nucleotide position of the band intensity of in vivo treated samples divided by the band intensity seen for in vitro UV treatment of naked genomic DNA. This procedure generates a fine-structure profile that gives information on in vivo chromatin structure. The profiles shown in Figure 4 confirm that HD11 cells and

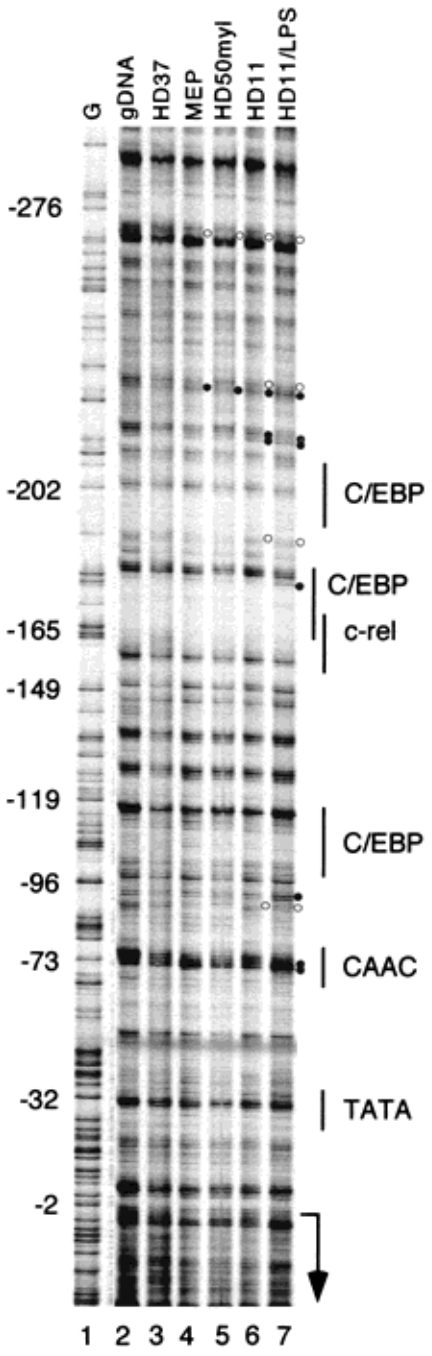

Figure 3. Photofootprinting of the chicken lysozyme promoter region by use of TDPCR. Primer set P130 was used to amplify the lower strand. UV dimer formation with naked DNA (gDNA, lane *2*) was compared with UV dimer formation in the cell lines indicated. A Maxam–Gilbert G-reaction was examined by LM–PCR using the same size linker and was run alongside for comparison. Previously identified in vitro transcription factor binding sites are indicated at the right. Diminished UV dimer formation as compared to naked DNA is indicated by an open circle, and enhanced reactivity is marked by a filled black circle with the position relative to the transcriptional start site indicated at the left.

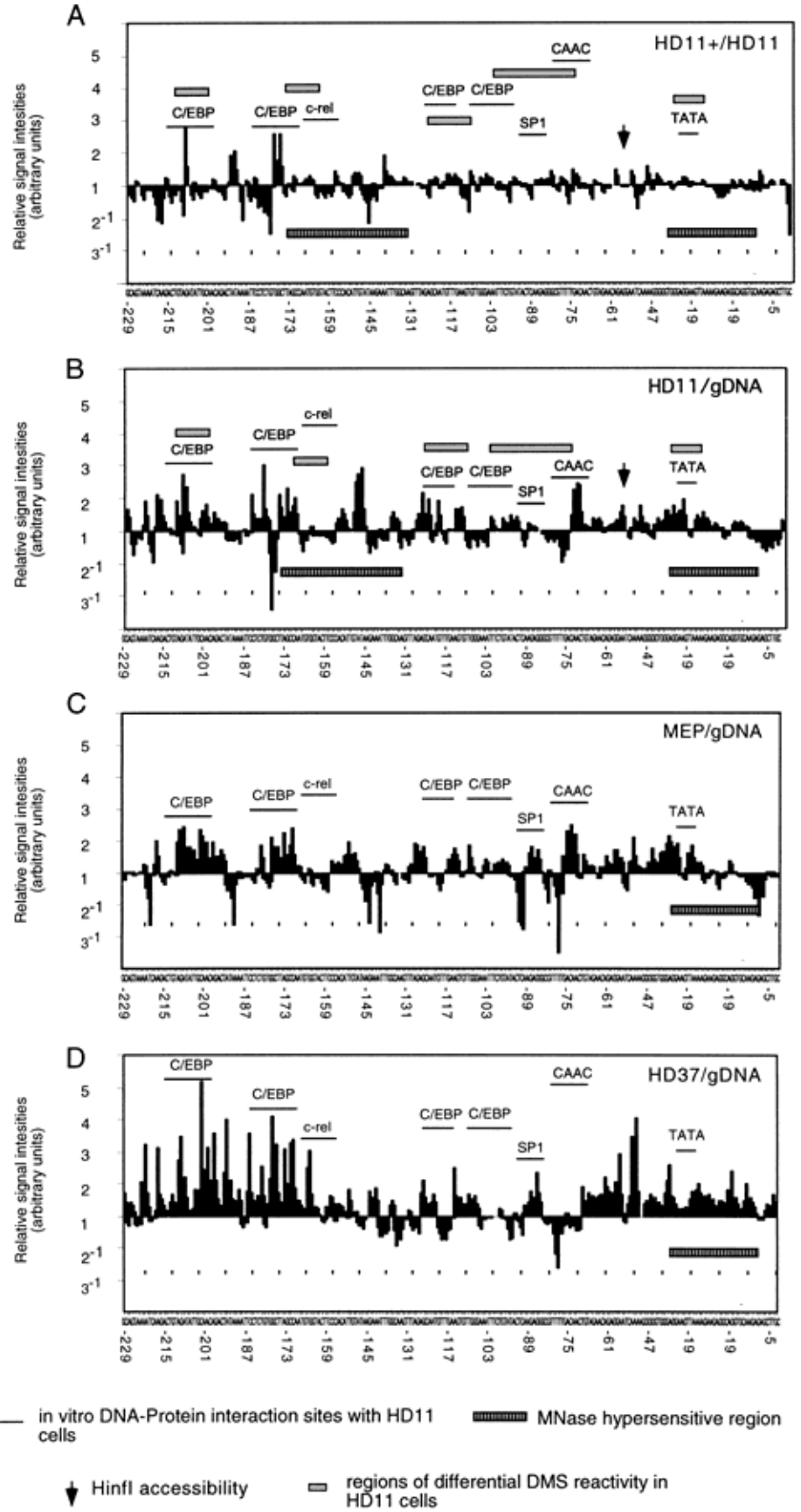

Figure 4. Chromatin fine-structure profiles of the lysozyme promoter. Values are the means of two independent and highly reproducible experiments (data not shown). The fluorescence of each band in the gel depicted in Figure 5 was individually quantified, and the signal intensity at each position was divided by the value of the band in the same position in UV-treated naked DNA (gDNA) or in vivo UV-treated DNA from the different cell lines as indicated.

HD50 MEP cells are more similar to each other than they are to HD37. Also worth noting is that for both HD11 and HD50 MEP there is a regular series of enhancements and protections of UV dimer formation for the region between –50 bp and –180 bp that could be wrapped DNA, as would be consistent with earlier MNase studies of this promoter (see Fig. 1). The patterns of MEP/genomic DNA and HD11/genomic DNA do show distinct differences from the pattern found in HD37 cells, but also there are some interesting similarities (in particular around the TATA and CAAC regions). We also obtained the same results with HD50 myl cells (data not shown). Several observations are noteworthy. The binding of transcription factors in HD11 cells only marginally alters the general UV footprinting pattern as compared to the precursor MEP cells. The appearance of DnaseI, Mnase, and restriction enzyme-accessible sites, which are thought to represent major changes in chromatin structure, correlates only with a change in the signal intensity for only a few specific bands over the transcription-factor binding sites such as the changes at the CAAC sequence or at –180 bp. It appears that the transcription factors do change the topology of DNA at some positions, but this change is superimposed on a basic pattern that is already present in MEPs. LPS stimulation of HD11 cells leads mainly to changes in UV lesion formation upstream of –150 bp, consistent with previous evidence indicating the existence of a LPS response element in this region (Phi van 1996). The latter result also confirms the reproducibility of our assay because all other signal differences fluctuate around the baseline. Many of the differences are somewhat less than twofold, consistent with previous data on the effect of nucleosome wrapping on photoreactivity (Gale et al. 1987). An important point is that the strikingly similar, clearly nonrandom profile seen in this region for HD50 MEP and HD11 provides strong evidence that the UV–TDPCR method combined with Li-Cor analysis can detect rather subtle changes. These and other experiments have established that the coefficient of variation for band intensities is usually about 10% for good primers that give adequately strong bands (Dai et al., unpubl.).

The similarity in basic chromatin structure between precursor cells (MEP) and expressing cells (HD11) is even more clear at the –6.1-kb enhancer (Fig. 5). This enhancer has been well characterized both by DNA–protein interaction studies and by functional assays (Theisen et al. 1986; Sippel et al. 1989; Grewal et al. 1992). In lysozyme nonexpressing cells the DNA is wrapped around a phased nucleosome that is remodeled after enhancer activation (Fig. 1; Huber et al. 1996). It has been shown to bind NFI proteins, an AP1-like protein, and C/EBP family members. On both strands a number of differences in UV dimer formation as compared to genomic DNA and HD37 cells are observed that are shared by all lysozyme-expressing cells and the multipotent precursors. Some UV footprints are visible that are unique for expressing cells, in particular with the lower strand. These include footprints that are localized outside the area of previously mapped DNA–protein interactions, indicating that the –6.1-kb lysozyme enhancer may have a more complex structure than previously thought.

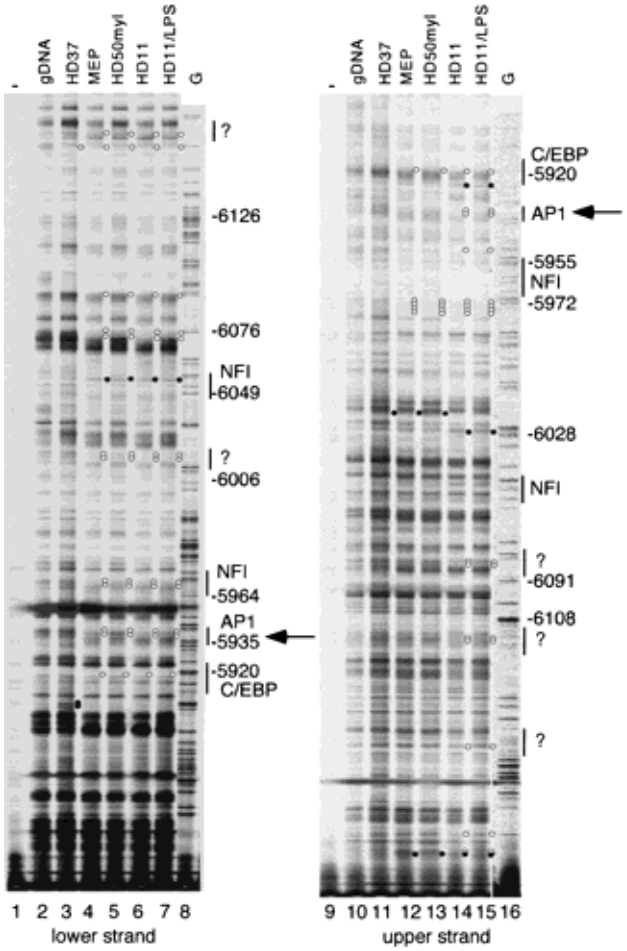

Figure 5. Photofootprinting of the –6.1-kb enhancer region (both strands). (*Left*) TDPCR with the D6.1U1 primer set that amplifies the upper strand. (*Right*) TDPCR with the U6.1MA primer set that amplifies the lower strand. UV dimer formation with naked DNA (gDNA, lanes *2,10*) was compared with UV dimer formation in the cell lines indicated. Both strands were analyzed. Lanes *7* and *15* represent HD11 cells treated for 24 hr with 5 µg/ml LPS. (Lanes *8,16*) A Maxam–Gilbert G-reaction was examined by LM–PCR using the same size linker and was run alongside for comparison. The scale indicates 10.3-bp distances. (Lanes *1,9*) Controls showing DNA samples not irradiated. Previously identified in vitro transcription factor binding sites are indicated at the right. (○) Diminished UV dimer formation as compared to naked DNA; (●) enhanced reactivity, with the position relative to the transcriptional start site indicated at the right. The position of the accessible *Hin*fI site is indicated as a black arrow.

The quantification of the UV footprinting experiments with the upper strand confirms what can be seen by eye (Fig. 6). The most important binding sites of the –6.1-kb enhancer as determined by functional assays (Grewal et al. 1992) are localized in a region that already is sensitive to MNase digestion in lysozyme nonexpressing cells, indicating that it may be internucleosomal linker DNA. Consistent with this notion, we observed a region up-

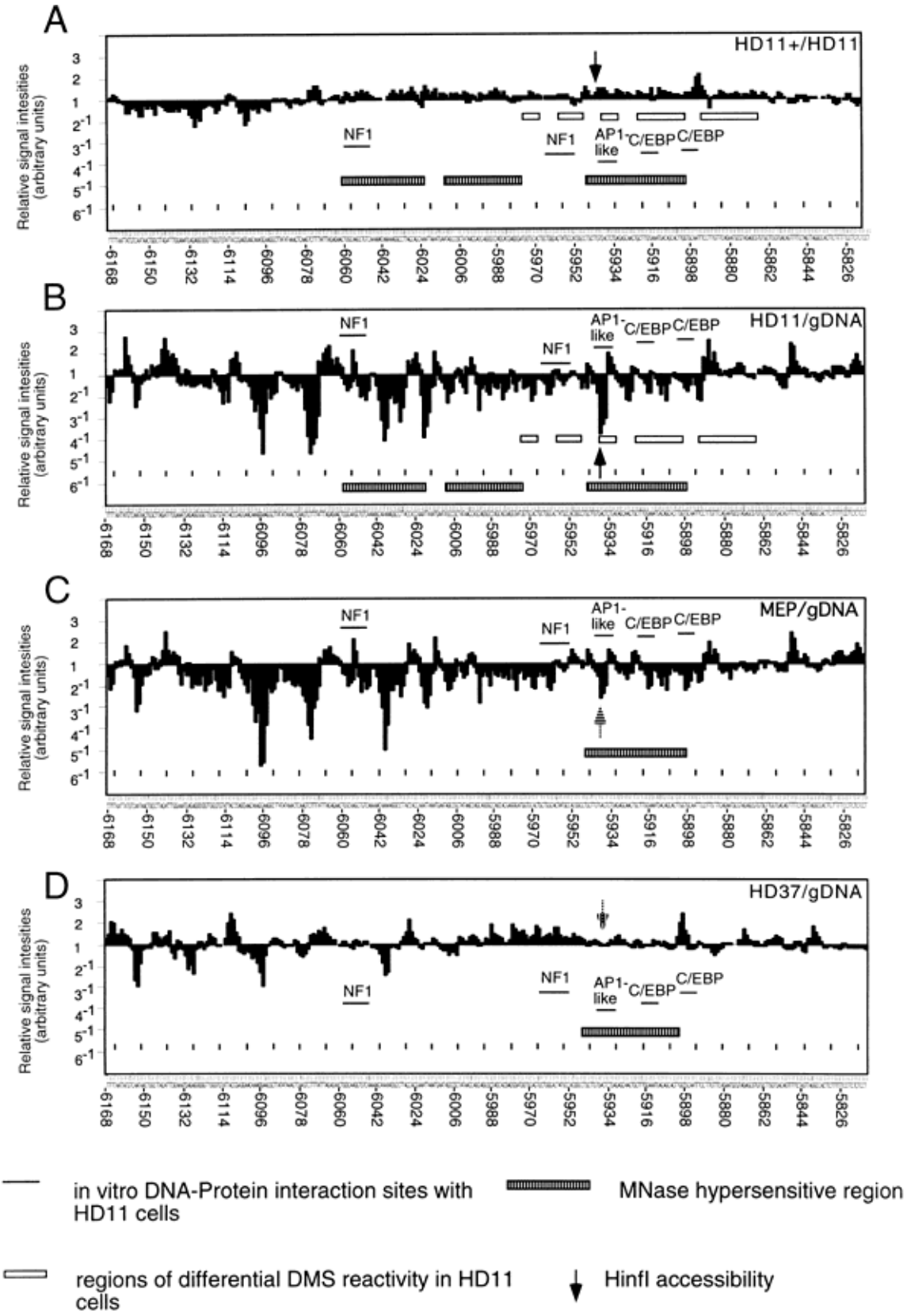

Figure 6. Chromatin fine-structure profiles of the –6.1-kb enhancer. Fluorescence of each band in the gel depicted in Figure 7 was individually quantified, and the signal intensity at each position was divided by the value of the band in the same position in UV-treated naked DNA (gDNA) or in vivo UV-treated DNA from the different cell lines as indicated. The scale indicates 10.3-bp distances.

stream of the enhancer core (5′ of –6024 bp) displaying a 10-bp periodicity and the presence of wrapped DNA. Again, aside from a few specific differences observed in lysozyme-expressing cells over the transcription-factor binding sites, the basic chromatin architecture of HD11 cells (± LPS) and HD50 MEP cells is highly similar. We obtained the same results analyzing HD50 myl and 1A1 cells (data not shown).

Lysozyme cis-regulatory elements do not bind trans-activator proteins in multipotent precursor cells

Given the above results an important question is, what factors are responsible for the establishment of a distinct chromatin pattern in multipotent precursor cells? Although no lysozyme mRNA can be detected in HD50 MEP cells, which are precursor cells not yet committed to the macrophage lineage (Huber et al. 1995; see also Fig. 7), we were interested to examine whether any of the transcription factors known to be crucial for early enhancer and promoter activity bind to these elements before the onset of transcription. Such in vivo potentiation of a specific gene locus, which represents a first step toward cell differentiation, was observed previously with the liver specific albumin enhancer (Gualdi et al. 1996). However, in this case it is not yet known whether this coincides with major chromatin rearragements.

We analyzed the lysozyme promoter (Fig. 7) using dimethylsulfate (DMS) methylation protection experiments that highlight purine [mostly G(N7)] contacts between proteins and DNA. To visualize regions of enhanced or suppressed DMS reactivity we used a new, simplified, and highly sensitive LM–PCR technique that uses a phosphorylated linker (see Materials and Methods). In addition to the G(N7) contacts mapped previously (Dölle and Strätling 1990), we were able to detect specific DNA–protein interactions upstream of the TATA box at –30 bp as well as at a previously unrecognized binding site upstream (around –270 bp) of the macrophage specific promoter elements at –200 bp. The majority of proteins binding to the lysozyme promoter recognize sequences characteristic for the C/EBP family of transcription factors (Fig. 7), which are known to play a major role in the regulation of myeloid specifically ex-

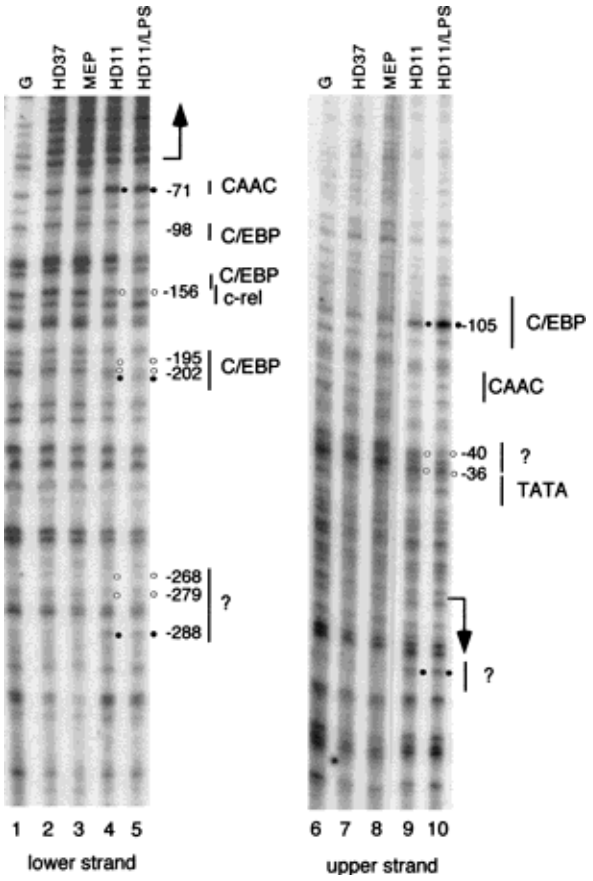

Figure 7. Dimethylsulfate (DMS) in vivo footprinting of the chicken lysozyme promoter. Differential DMS reactivity with naked DNA (lanes *1,6*) was compared with DMS reactivity of DNA in the cell lines indicated. Both strands were analyzed. (*Left*) LM–PCR with primer set P351 that amplifies the lower strand. (*Right*) LM–PCR with primer set P1 that amplifies the upper strand. The transcription start site is indicated by an arrow. Previously identified in vitro transcription factor binding sites are indicated at the right. (○) Diminished DMS reactivity as compared to naked DNA; (●) enhanced reactivity, with the position relative to the transcriptional start site indicated at the right.

pressed genes (for review, see Tenen et al. 1997). In accordance with these observations, we demonstrated that overexpression of C/EBP proteins trans-activate the chicken lysozyme promoter (data not shown). In addition, our study demonstrates that one of the C/EBP footprints at –105 bp is LPS inducible. Since HD50 MEP cells do not express C/EBP proteins (Katz et al. 1993), it is not surprising that C/EBP specific in vivo contacts over these binding sites were absent. No other G(N^7) contact can be mapped in these cells; the DMS reactivity pattern is identical to that observed in HD37 erythroblast cells and genomic DNA.

The finding that the transcription factors important for enhancer activity occupy their binding sites in vivo only in expressing cells could also be confirmed at the –6.1 kb enhancer (Fig. 8, lanes 6,7,14–16). In this context, it is noteworthy that extreme DMS hyperreactivity of one of the central Gs of the palindromic NFI binding site is only apparent on the upper strand, and this may indicating a strong, asymmetric distortion of DNA structure.

Gene expression correlates with the establishment of a stable chromatin structure

It is now well established that the acetylation state of the histone amino termini is one parameter determining the topology of DNA within the nucleosome (Norton et al. 1989; Li et al. 1999) and the inheritance of chromatin structure; for example, the polycomb group of proteins associate with histone deacetylases (HDAC; van der Vlag and Otte 1999). In addition, a growing number of transcription factors as well as architectural factors have been identified whose activity is regulated by acetylation (Kouzarides 2000). To investigate the effects of increased acetylation on chromatin photofootprints, we cultured our HD11 cells, HD50 MEP cells, and HD37 cells in the

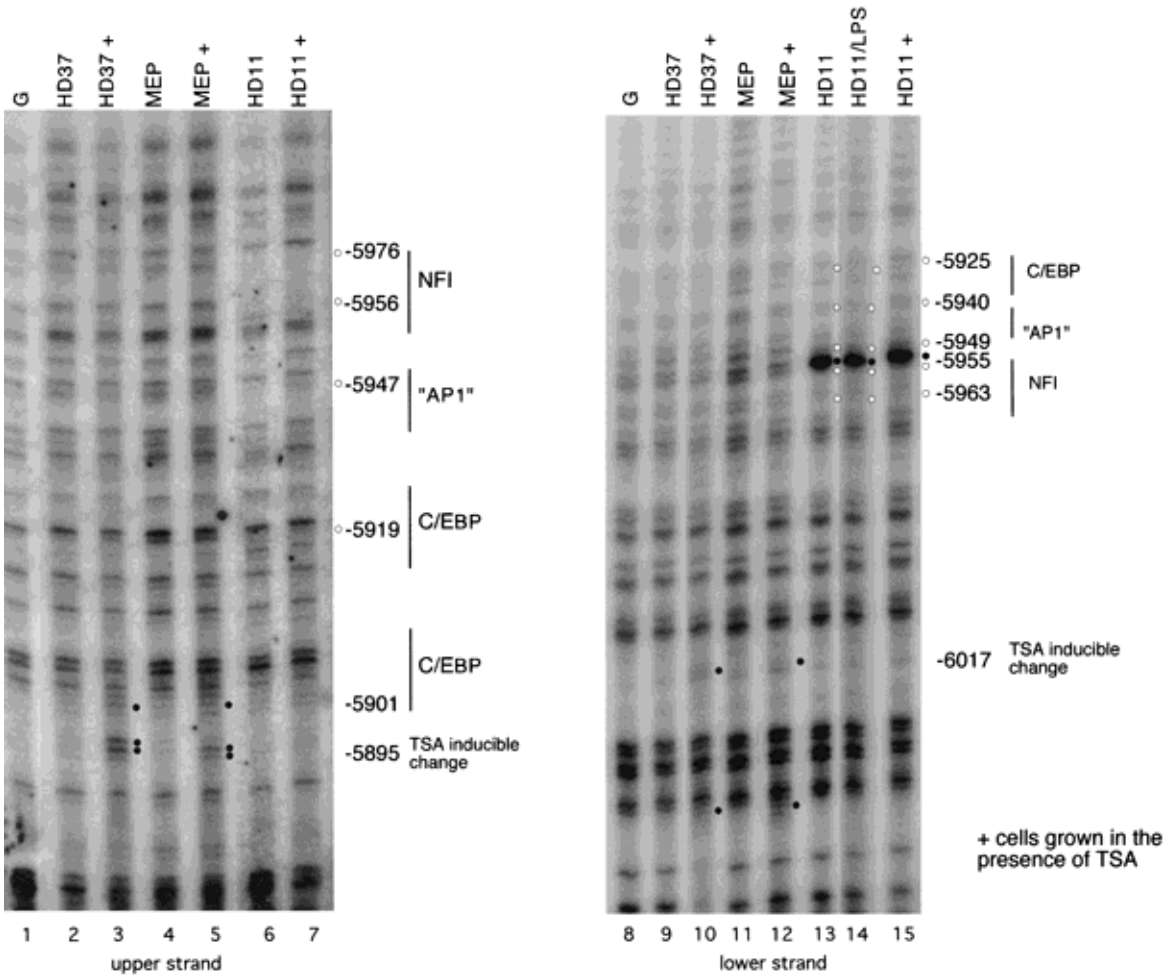

Figure 8. Dimethylsulfate (DMS) in vivo footprinting of the –6.1-kb enhancer. DMS reactivity with naked DNA (lanes *1,8*) was compared with DMS reactivity in the cell lines indicated. Both strands were analyzed. (*Left*) LM–PCR with primer set D6.1U1 that amplifies the upper strand. (*Right*) LM–PCR with primer set U6161 that amplifies the lower strand. (Lanes *5,10*) HD11 cell treated for 24 hr with 5 μg/ml bacterial lipopolysaccharide (LPS). Previously identified in vitro transcription factor binding sites are indicated at the right. (+) Cells grown in the presence of 100 nM/ml Trichostatin A (TSA). (○) Diminished DMS reactivity as compared to naked DNA, (●) enhanced reactivity, with the position relative to the transcriptional start site indicated at the right.

presence or absence of 100 nM of the histone deacetylase inhibitor Trichostatin A (TSA) and determined changes in lysozyme expression and chromatin structure. For comparison, we also examined embryonic fibroblasts and macrophages from a transgenic mouse line that carries ~100 copies of the chicken lysozyme transgene (Bonifer et al. 1994). Figure 9 shows that TSA upregulates lysozyme expression in HD11 cells as well as in mouse macrophages but has no effect on HD37 or HD50 MEP cells, which show no trace of lysozyme RNA.

We examined the effect of TSA treatment on both –6.1-kb and –3.9-kb early enhancers of the lysozyme locus. Surprisingly, an effect of TSA was observed in the DMS footprint for both, leading to an increased reactivity at A residues. In the –6.1-kb enhancer, TSA-induced adenosine specific methylation enhancements at –5895 bp and –6017 bp can be seen in both lysozyme nonexpressing cell types (Fig. 8, MEP and HD37) but not in HD11 cells. Interestingly, these A residues are located within an AT-rich sequence flanking the enhancer core, from which we know that it most likely represents internucleosomal linker DNA (Huber et al. 1996).

The recently investigated –3.9-kb enhancer has a different structure than the –6.1-kb enhancer, being organized in specifically positioned nucleosomes only in lysozyme-expressing cells, as determined by MNase mapping (Kruger et al. 1999; Fig. 1). In lysozyme nonexpressing cells (HD37, HD50 MEPs, and transgenic mouse embryonic fibroblasts), nucleosomes occupy alternate positions, one of which is stabilized after enhancer activation and DHS formation (Huber et al. 1996; Kruger et al. 1999). This element is therefore particularly suited to determine to which extent basic chromatin structure has developed toward the active pattern. Here, we examined not only the chromatin from chicken cell lines but also the chromatin from macrophages and embryonic fibroblasts generated from the transgenic mouse line.

In lysozyme-expressing cells, the –3.9-kb enhancer is recognized by members of the NFI factor family and several factors that are not yet fully characterized (Kruger et al. 1999) and whose role in enhancer activation will be published elsewhere. Clear DMS footprints of the upper strand are seen in Figure 10A, and these are over transcription-factor binding sites in lysozyme expressing cells. Treatment with TSA does not change this basic pattern. In HD37 cells and to some extent also in HD50 MEP cells, adenosine-specific hypermethylations in an AT-rich region downstream of the NFI site are observed at –3796 bp and at –3776 bp, and these are enhanced after TSA treatment. Again, this region most likely represents internucleosomal linker DNA (Huber et al. 1996; Kruger et al. 1999). This element in primary mouse macrophages binds the same set of transcription factors that it does in chicken cell lines, confirming our earlier observations that the regulation of the lysozyme locus in both chicken cell lines and primary mouse cells is highly similar (for review, see Bonifer et al. 1996). The protections are somewhat weaker in the mouse cells, which can be explained by the multicopy nature of the transgene. Although originally being expressed in a copy-number-dependent fashion (Bonifer et al. 1994), not all copies may be simultaneously occupied at a given time because we have observed some silencing of the transgene array over the years (C. Bonifer, unpubl.).

Photofootprinting experiments (Fig. 10B) revealed a number of subtle changes in UV dimer formation in lysozyme-expressing cells around the transcription factor binding sites, both in HD11 cells and mouse macrophages.

In the nonexpressing HD37 cells and mouse embryonic fibroblasts, the AT-rich region around –3805 bp shows a higher frequency of UV dimer formation compared to genomic DNA. This pattern does not significantly change after TSA treatment. In HD50 MEP cells, HD11 cells, and mouse macrophages, this region is protected from UV lesion formation. The pattern of HD11 cells and mouse macrophages remains so after TSA treatment. However, in HD50 MEP cells, the UV dimer formation pattern is changed to resemble that of HD37 cells.

Taken together, our observations show that a basic active chromatin structure is already in place in HD50 MEP, the multipotent progenitor cells. TSA can perturb this basic chromatin pattern, but only in lysozyme nonexpressing cells. Once trans-activating factors have bound and an active enhancer complex has been established, as in HD11 cells, the pattern is resistant to TSA treatment, a result consistent with the mature enhancer already being organized in hyperacetylated chromatin.

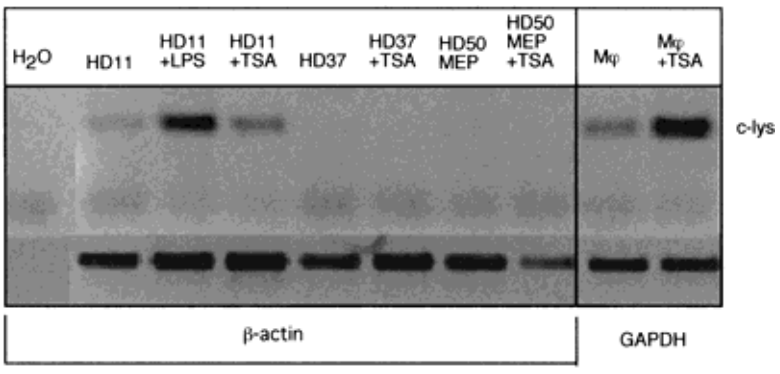

Figure 9. Effect of trichostatin A (TSA) on lysozyme expression. RT–PCR was performed with RNA prepared from TSA treated and nontreated chicken and mouse macrophage cells as indicated, using lysozyme-specific, chicken β actin–specific, and mouse GAPDH–specific primers. For comparison, expression was assayed HD11 cells treated for 24 hr with 5 μg/ml LPS.

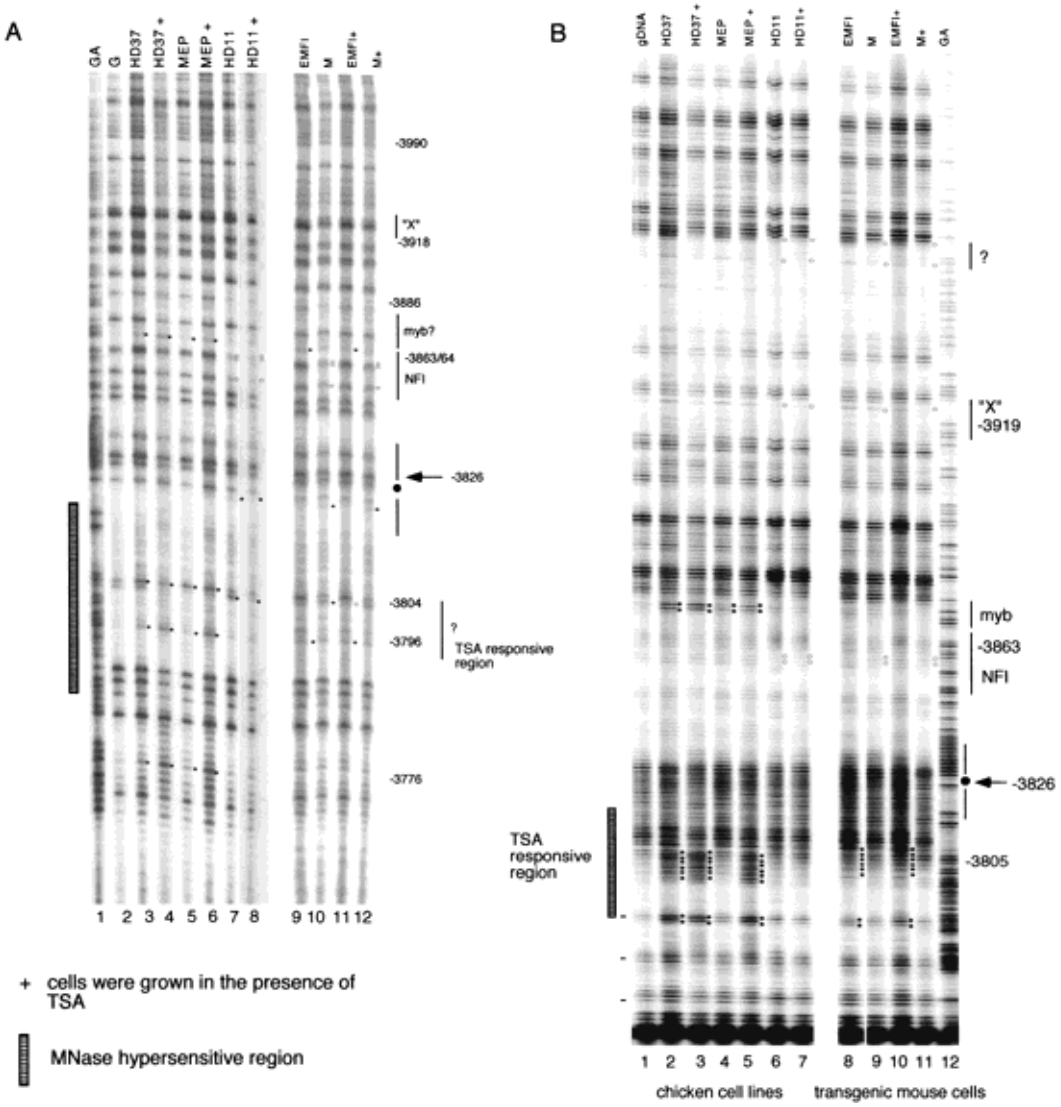

Figure 10. In vivo footprinting analysis of the –3.9-kb enhancer. The chicken cell lines used (HD37, HD50 MEP, and HD11) are shown at the top, as are the transgenic mouse primary cell lines: (M) mouse macrophages; (EMFI) embryonic mouse fibroblasts. The position of an accessible *Hin*fI site over an AT-rich palindromic sequence is indicated as a black arrow. The hatched bar indicates a region of preferential MNase cleavage in lysozyme expressing cells. (+) Cells grown in the presence of 100 nM Trichostatin A (TSA). Previously identified in vitro transcription-factor binding sites are indicated at the right. (*A*) Dimethylsulfate (DMS) footprinting. Naked DNA (Maxam–Gilbert G and G+A; lanes *1*,*2*) was compared with the chicken cell lines (lanes *3*–*8*) and the primary transgenic mouse cells (lanes *9*–*12*). LM–PCR was done with primer set D376, which amplifies the upper strand. (○) Diminished DMS reactivity as compared to naked DNA; (●) enhanced reactivity, with position relative to the transcriptional start site indicated at the right. (*B*) UV Photofootprinting of the –3.9-kb enhancer region. Naked DNA (gDNA, lane *1*) was compared with DNA from the chicken cell lines (lanes *2*–*7*) and the primary transgenic mouse cells (lanes *8*–*11*) TD–PCR was with primer set D376, which amplifies the upper strand. Lane *12* shows a Maxam–Gilbert G+A reaction examined by LM–PCR, using a linker to give the same size as for TD–PCR. (○) Diminished UV dimer formation as compared to naked DNA; (●) enhanced reactivity, with position relative to the transcriptional start site indicated at the right.

Discussion

The role of chromatin architecture in the developmental activation of the lysozyme locus

Our previous experiments in transgenic mice and chicken cell lines clearly demonstrated a close link between the structural activation of the different enhancers on the lysozyme locus at specific developmental stages and their ability to interact with the promoter and activate transcription (Jägle et al. 1997; Huber et al. 1997). The experiments described in this study provide the basis for a more detailed understanding of the changes leading to gene locus activation during myeloid differentiation, helping to link the step-

wise transcriptional activation of the chicken lysozyme locus to a precisely timed and specific reorganization of chromatin structure (for review, see Bonifer et al. 1997).

Our high-resolution quantitative UV-footprinting experiments have generated fine-structure profiles of the different cis-regulatory elements that indicate all changes in DNA structure that occurred as a result of differential folding by different factors. Although with photofootprinting it is difficult to distinguish transcription factor–generated distortions of DNA structure for chromatin-generated distortions, this method adds a powerful tool for examination of subtle changes of chromatin during development.

We obtained a number of important details about the chromatin architecture of promoter and –6.1-kb enhancer and the way a stable enhancer and promoter complex is established. The major transcription factors binding to the lysozyme promoter in macrophages are members of the C/EBP factor family, most likely C/EBP β (NF-M). These factors and c-rel are responsible for the upregulation of the lysozyme promoter during LPS-induced macrophage activation (Goethe and Phi van 1994; Phi van 1996). The UV lesion pattern we observed is consistent with the notion that the LPS responsive element is located upstream of –150 bp, as suggested earlier (Phi van 1996). However, we also observed an LPS responsive footprint over a C/EBP binding site, indicating that these factors contribute to the upregulation of the lysozyme promoter after LPS treatment. Our previous MNase analyses suggested that these factors encounter a positioned nucleosome in lysozyme nonexpressing cells that is remodeled after promoter activation (Huber et al. 1996). Changes in accessibility seen earlier for DNaseI and MNase (Huber et al. 1995, 1996) have been confirmed by the *Hin*fI restriction enzyme accessibility assay reported here.

The deletion of the –6.1-kb enhancer leads to a delay in the onset of transcription, highlighting that this element is vital for lysozyme locus activation at the correct developmental stage (Jägle et al. 1997). In vivo, the –6.1-kb enhancer is bound by C/EBP family members, together with members of the NFI factor family and an AP1-like protein. However, here it appears as if the binding sites of the factors of which the enhancer core consists are arranged within linker DNA between two phased nucleosomes. The central NFI binding site is located in a region displaying no periodicity of UV dimer formation and is sensitive to MNase in lysozyme nonexpressing cells (see Fig. 2B). This is interesting because NFI binding is dependent on chromatin remodeling activities (Di Croce et al. 1999) and is inhibited if the binding site is organized in a phased nucleosome (Pina et al. 1990; Blomquist et al. 1996). Together with the C/EBP factors and AP1 this may therefore be an efficient initiation complex for the activation of gene expression. However, we are aware of the fact that further structural studies are necessary to examine the precise role of nucleosomes in the formation of enhancer and promoter complexes.

The formation of an active chromatin structure can occur in the absence of the binding of trans-activators

All chromatin analyses performed at the resolution of Southern blots failed to detect a difference between the chromatin structure of the lysozyme locus in multipotent progenitor cells and other lysozyme nonexpressing cells. This holds true for DHS and MNase mapping as well as for the *Hin*fI accessibility assays presented here. This distinguishes our experiments from previous studies that detected major chromatin rearrangements on differentiation specific genes in hematopoietic progenitor cells (Jiménez et al. 1992; Yoo et al. 1996). However, these major chromatin rearrangements coincided with the detection of a low level of transcription of these genes in these cells (see also below; Hu et al. 1997). The photofootprinting study reported here with the lysozyme locus provides for the first time clear evidence for a maturation of chromatin architecture toward the active pattern even earlier in hematopoiesis. Specific nucleoprotein complexes are already in place in multipotent precursor cells that do not transcribe the gene and do not show trans-activating factors binding to lysozyme cis-regulatory elements. We observed the same chromatin fine-structure pattern in several different cell types, which have in common only that they belong to the myeloid lineage. We have also seen the same pattern for two other cell lines (data not shown): HD50 myl and 1A1 cells, which were derived from a different MEP precursor cell clone. All three cell lines grow in suspension. We also saw the same pattern in HD11 cells that were derived from monocytes transformed with a different oncogene (*c-myc*), were isolated from peripheral blood of an adult animal, and grew as adherent cells. LPS-stimulated HD11 cells represent activated macrophages that are terminally differentiated and have ceased to grow. In addition, our preliminary experiments indicate a similar pattern in primary cells of transgenic mice. We therefore conclude from these experiments that the similarity in the UV footprinting pattern we observe represents a potentiated chromatin state and is a hallmark of genes with the potential to be expressed or that are expressed in the myeloid lineage.

One conclusion we draw is that this potentiated chromatin structure can be established in the absence of transcription and without the continuous binding of the transcription factors necessary for lysozyme expression in mature macrophages. DMS and UV footprints characteristic of factor binding as seen in later stages are not seen in MEP cells. Since our DMS footprinting assays rely on modifications introduced into purine residues, the formal possibility exists that we might miss binding of factors not making any G(N7) contacts. However, we regard it as unlikely that a stable protein–DNA complex is formed on the cis-elements that are invisible to both DMS and UV in all elements examined. Moreover, although C/EBP proteins are not expressed in MEP cells, other factors like NFI are present (data not shown). Our findings rather point toward a major role of a different set of nonhistone proteins acting with or on nucleosomes to

establish a distinct chromatin pattern that then is maintained through several cell divisions and subsequent stages of differentiation in the myeloid pathway. Likely candidates for factors involved in this process are histone acetylases/de-acetylases (HACs and HDACs), SWI/SNF type complexes, and vertebrate members of the polycomb group of proteins.

A wealth of evidence shows a correlation between transcriptional activity and the histone modification state of specific genes (for review, see Struhl 1998). The histone acetylation level clearly distinguishes gene coding regions from centromeric and telomeric heterochromatic regions independent of the expression level, however, in a differentiation-dependent fashion (O'Neill and Turner 1999). HDACs as well as HATs display site-specific activities (Rundlett et al. 1998; Zhang et al. 1998). Therefore, a hypothesis has been put forward that states that different types of covalent modifications of histone tails consist of a stable "histone code," which is read by interacting factors responsible for downstream events (Strahl and Allis 2000). Our TSA experiments indicate that the reactivity of DNA toward modifying agents can be perturbed by histone hyperacetylation. Interestingly, in both the –6.1-kb and to some extent also with the –3.9-kb enhancer this also holds true for DMS reactivity. As nucleosomes were up to now thought to be transparent for DMS reactivity, this would point to the binding of an acetylation responsive transcription factor as it has been suggested in similar experiments carried out with butyrate-treated cells that revealed TSA-dependent G(N7) reactivities at specific sites (Ikuta et al. 1998). However, taking our UV footprinting and MNase experiments into account, enhanced DMS reactivity may also be caused by a change in the topology of DNA, as suggested in Li et al. (1999).

In *Drosophila*, and most likely also in other organisms, members of the polycomb (Pc) group of proteins are involved in the repression of gene activity. Another group of proteins, members of the trithorax (Trx) family, including *Drosophila* homologs of the yeast SWI/SNF complexes (Cairns 1998), are involved in the maintenance of the active state. The function of both Pc and Trx proteins seems to be in the epigenetic mechanisms for the maintenance of cell memory, that is, the preservation of determined states during subsequent development. Once established, the active or repressed state is stably maintained in a wild-type Pc and Trx environment. Strikingly, the continuous presence of the initial repressor or trans-activator is not needed (Cavalli and Paro 1999). Support for the idea that histone modification may be involved in the establishment of such an epigenotype comes from the same study, which presented evidence for histone acetylation being a key component of the heritable tag for an activated regulatory element.

The role of transcription factors in the establishment of an active chromatin structure

The question remains, How is the potentiated chromatin state that we observe in HD50 MEP precursor cells established in the first place, and what role do transcription factors play in this process? One possibility is that transcription factors that cooperate with chromatin remodeling complexes are transiently recruited to their binding sites (possibly after replication) and initiate a chromatin modification event. We hypothesize that in precursor cells that, due to their developmental state, do not yet express the requisite transcription factor combination, no stable cis-regulatory complexes can be formed that drive transcription. This would also imply that chromatin reorganization during development is not entirely determined by transcription factors driving gene expression, providing a molecular explanation for the apparent lack of major effects of deletions of important regulatory elements on general chromatin structure of a natural gene, as exemplified by experiments examining a deletion of the locus control region in the β-globin locus (Bender et al. 2000).

Basic chromatin structure can not be disturbed by TSA treatment in lysozyme expressing cells (HD11 cells and mouse macrophages), in contrast to lysozyme nonexpressing cells. Because both histones and nonhistone proteins can be the target of acetylases, we can only speculate on the nature of the nucleoprotein complexes on which HATs and HDACs act. It will be of interest to focus in on the "TSA-responsive" regions in future work, using in vitro and chromatin immunoprecipitation methods to find out details of the protein and nucleosomal changes involved. However, our data are clearly consistent with the idea that once the right transcription factor combination is present, a stable chromatin structure is established. Stable transcription factor complexes consisting of a large number of interacting factors will recruit the same type of chromatin-remodeling activities after each round of replication and will consistently establish the same chromatin modifications. In contrast, lysozyme nonexpressing cells may still require the dynamic equilibrium of both HAT and HDAC activities to maintain their respective chromatin patterns. However, each cell line has a different nucleosome–nonhistone protein complex on each cis-regulatory element, the fine structure of which can be distinguished by the methods used here. Future experiments will be aimed at elucidating which factors make up these complexes. Taken together, our experiments indicate a developmental maturation of chromatin structure setting the stage on which transcription factors can act.

Experiments have been described that suggest a lineage promiscuity of multipotent hematopoietic precursor cells with respect to the expression of markers of differentiated cells (Hu et al. 1997). Commitment to different cell lineages was interpreted as a repression of genes specific for the respective other lineages during differentiation (Cross and Enver 1997). Genes like the chicken lysozyme gene that are not yet expressed in immature precursor cells may exist in a potentiated chromatin state that is further modified during cell differentiation. To this end, it will be very interesting to unravel the hierarchical relationship of the epigenetic states of

the lysozyme locus in different cell lineages both inside and outside the hematopoietic system.

Materials and methods

Cell culture

HD50 MEP, HD50 myl, 1A1, HD37, and HD11 cells (Graf et al. 1992) were grown in Iscove's modified DMEM medium (Life Technologies) supplemented with 8% fetal calf serum and 2% chicken serum, 100 U/ml penicillin, 100 µg/ml streptomycin, 292 µg/ml L-Glutamine, and 0.15 mM monothioglycerol. The transgenic mouse line carrying construct XS (Bonifer et al. 1994) was kept as a homozygous line in our own mouse colony. Cells from the peritoneal cavity were taken in culture in standard Iscove's medium supplemented with 10% fetal calf serum (FCS) and 10% L-cell conditioned medium for 16 hr (Bonifer et al. 1990). Embryonic fibroblasts were prepared from mouse embryos 12 days after fertilization as described earlier (Huber et al. 1994). When indicated, the cells where stimulated with 5-µg/ml bacterial lipopolysaccharide (LPS; Sigma) for 24 hr or treated with 100 nM of the histone deacetylase inhibitor trichostatin A (TSA; Sigma) for 48 hr.

Restriction enzyme accessibility assays

For restriction enzyme accessibility assays, cells where treated for 1–2 min at room temperature in permeabilization buffer (7.5 mM Tris-HCl at pH 7.5, 30 mM KCl, 7.5 mM NaCl, 2.5 mM $MgCl_2$, 0.25 mM EDTA, 150 mM sucrose, 0.25 mM β-mercaptoethanol, 0.005% lysolecithin), washed with phosphate buffered saline (PBS; Life Technologies) and then digested with 100 U *Hin*fI in the corresponding reaction buffer (Life Technologies) for 1 hr at 37°C. Cells were lysed in buffer (65 mM NaCl, 10 mM Tris-HCl at pH 8, 7.5 mM EDTA, 1% w/v SDS, and 600 µg/ml Proteinase K) and DNA was analyzed by Southern blot after digestion with *Eco*RI.

In vivo footprinting analysis

DMS treatment and ligation-mediated PCR (LMPCR). Cells were treated with 0.2% DMS in PBS for 5 min at room temperature. DMS reaction was stopped by addition of ice-cold PBS, followed by two washes with PBS. Cells were lysed in lysis buffer overnight at room temperature and DNA was purified. In vitro DMS treatment of naked DNA was performed essentially as described by Maxam and Gilbert (1980). DNA was treated with Piperidine at 0.1 M for 10 min at 90°C, followed by three lyophilizations in water. Cleavage sites were analyzed by LM–PCR. LM–PCR was carried out as described (Hershkowitz and Riggs 1997) with the following modifications: biotinylated primers were used for the first primer extension, which was carried out using Vent exo-DNA polymerase (New England Biolabs). Primer extension products were ligated to linker LP25–21, which consists of a 25mer (GCGGTGACCCGGGAGATCTGAATTC) annealed to a 21mer (GAATTCAGATCTCCCGGGTCA). The 21mer was 5′ phosphorylated by T4 polynucleotide kinase (New England Biolabs) before annealing. After ligation, specific biotinylated products were isolated on streptavidin paramagnetic beads (DYNAL) and used for PCR amplification using a nested specific primer and the 25mer. Primer extension and PCR conditions were optimized for each primer set. PCR products were labeled by primer extension using ^{32}P-labeled nested primers and were analyzed on 6% denaturing polyacrylamide gels.

UV irradiation and terminal transferase polymerase chain reaction (TDPCR). Cells were irradiated in UV stratalinker model 2400 (Stratagene) at 1000 J/m^2 and lysed and DNA was purified. Naked DNA was irradiated at 1000 J/m^2 in 5-µl drops. DNA was analyzed by TDPCR essentially as described (Komura and Riggs 1998) with the following modifications. Biotinylated primers were used for the first primer extension, and products were isolated on streptavidin paramagnetic beads and treated with terminal deoxynucleotidyl transferase as described. The linker used for ligation was linker γ described in Komura and Riggs (1998) consisting of a 27mer (dGCGGTGACCCGGGAGATCTGAATTCCC) and a 24mer (dAATTCAGATCTCCCGGGTCACCGC) that carries an aminopentyl blocking group at the 3′ end. The 24mer was 5′ phosphorylated by T4 polynucleotide kinase before annealing. PCR-amplified products were labeled by primer extension using ^{32}P-labeled or fluorescent (LI-COR) nested primers. Labeled primer extension reactions were analyzed on 6% polyacrylamide gels. LI-COR gels were quantified using the Scanalytics RFLP image analysis program.

Oligonucleotides. Sequences of the oligonucleotides used as primers for LMPCR or TDPCR analysis and the corresponding nucleotide numbers (relative to the transcriptional start site of the chicken lysozyme gene) were: U6.1MA (–6290) (dATCCCTACTGTGCCGTCCTGGT) (–6269), U6.1MA3 (–6277) (dCCTGGTTTTACGTTACCCCCTGAC) (–6250), U6.1MB (–6255) (dCCTGACTGTTCCATTCAGCG) (–6235), D6.1U1 (–5766) (dGAACGTTCACTTGACTGGGAT) (–5786), D6.1U2 (–5778) (dGACTGGGATTACCAGCATGGAGAC) (–5801), D6.1U3 (–5788) (dGGAGACATGCTTAGGAGAATG) (–5816), U6161 (–6142) (dAGATTGGAAATGAGAGGGGG) (–6122), U6162 (–6136) (dGGAAATGAGAGGGGGTTGGGT) (–6116), U6163 (–6131)(dTGAGAGGGGGTTGGGTGTATT) (–6111), D376 (–3716) (dGAGCTACACAACCCTTCAGC) (–3735), D376A (–3732) (dCAGCTGTCTCTCCCTTGATGG) (–3755), D376B (–3748) (dGATGGCAGCCTGCCCCACAAG) (–3768), P1301 (+141) (dAGTTATCAAGTCCGTGACGCTTCATAG) (+115), P1302 (+123) (dGCTTCATAGCCGCTGCCAGCTCACATC) (+97), P1303 (+111) (CTGCCAGCTCACATCGTCCAAAGACTTTC) (+83), P351 (–366) (dTTCAGCACTTGCGAAGAAGAG) (–346), P352 (–355) (dGCGAAGAAGAGCCAAATTTGC) (–336), P353 (–346) (dGCCAAATTTGCATTGTCAGGA) (–326), P1 (+37) (dGACCTCATGTTGCCAGTGTCG) (+17), P2 (+24) (dCAGTGTCGTACACACAGCGGG) (+5), and P3 (+15) (dACACACAGCGGGACTGCAAGC) (–6). Primers U6.1MA, D6.1U1, U6161, U42A, D376, P1301, P351, and P1 were biotinylated. Sets of three are used for each TDPCR experiment, for example, U6.1MA (–6290), U6.1MA3 (–6277), and U6.1MB (–6255). The first primer is for primer extension, the second for PCR, and the third for the labeling reaction.

RT–PCR

Total RNA was prepared using Trizol (Life Technologies) according to the manufacturer's instructions. cDNA synthesis from 1-µg RNA samples was carried out using random hexamers as primers and Moloney murine Leukemia Virus reverse transcriptase (Life Technologies) in a reaction volume of 20 µl under conditions recommended by the manufacturer. Primer pairs used for PCR analysis of the cDNAs were: Chicken lysozyme (ch-lys): dGATCGTCAGCGATGGAAACGGC and CTCACAGCCGGCAGCCTCTGAT-3′, chicken β-actin: dTCCACCGCAAATGCTTCTAAAC and TCTATCACTGGGGAACACAGCC; and mouse GAPDH: dGGTCATCATCTCCGCCCCTTCTGC and GAGTGGGAGTTGCTGTTGAAGTCG. PCRs were performed in a total volume of 30 µl using 1.5 U *Taq*

polymerase (Promega). Initial denaturation step at 95°C for 2 min was followed by 30 cycles of 95°C for 40 sec, annealing temperature for 1 min, 72°C for 1 min, and a 10-min final elongation step at 72°C. Annealing temperatures for the chicken lysozyme primers were 62°C and 60°C for the chicken β-actin and mouse GAPDH primers, respectively.

Acknowledgements

We thank A. Markham, P. Cockerill, P. Robinson, and J. Frampton for corrections and critical comments on the manuscript. This work was supported by grants from the Wellcome Trust and the BBSRC to C.B. and National Institutes of Health grant RO1 GM50575 to A.D.R.

The publication costs of this article were defrayed in part by payment of page charges. This article must therefore be hereby marked "advertisement" in accordance with 18 USC section 1734 solely to indicate this fact.

References

Altschmied, J., Müller, M., Baniahmad, S., Steiner, S., and Renkawitz, R. 1989. Cooperative interaction of chicken lysozyme enhancer sub-domains partially overlapping with a steroid receptor binding site. *Nucleic Acids Res.* **17:** 4975–4991.

Becker, M.M. and Grossmann, G. 1993. Photofootprinting DNA in vitro and in vivo. In *Footprinting of nucleic acid-protein complexes.* pp. 129–159. Academic Press, New York, NY.

Becker, M.M. and Wang, J.C. 1984. Use of light for footprinting of DNA in vivo. *Nature* **309:** 682–687.

Bender, M.A., Bulger, M., Close, J., and Groudine, M. 2000. β-globin gene switching and DNaseI sensitivity of the endogenous β-globin locus in mice do not require the locus control region. *Mol. Cell* **5:** 387–393.

Beug, H., von Kirchbach, A., Döderlein, G., Conscience, J.-F., and Graf, T. 1979. Chicken hematopoietic cells transformed by seven strains of defective avian leukemia viruses display three distinct phenotypes of differentiation. *Cell* **18:** 375–390.

Blomquist, P., Li, Q., and Wrange, O. 1996. The affinity of nuclear factor I for its DNA site is drastically reduced by nucleosome organization irrespective of its rotational or translational position. *J. Biol. Chem.* **271:** 153–159.

Bonifer, C., Vidal, M., Grosveld, F., and Sippel, A.E. 1990. Tissue specific and position independent expression of the complete gene domain for chicken lysozyme in transgenic mice. *EMBO J.* **9:** 2843–2848.

Bonifer, C., Yannoutsos, N., Krüger, G., Grosveld, F., and Sippel, A.E. 1994. Dissection of the locus control function located on the chicken lysozyme gene domain in transgenic mice. *Nucleic Acids Res.* **22:** 4202–4210.

Bonifer, C., Huber, M.C., Faust, N., and Sippel, A.E. 1996. Regulation of the chicken lysozyme locus in transgenic mice. *Crit. Rev. Eukaryot. Gene Expr.* **6:** 285–297.

Bonifer, C., Jägle, U., and Huber, M.C. 1997. The chicken lysozyme locus as a paradigm for the complex regulation of eukaryotic gene loci. *J. Biol. Chem.* **272:** 26075–26078.

Cairns, B.R. 1998. Chromatin remodelling machines: Similar motors, ulterior motives. *TIBS* **23:** 20–25.

Cavalli, G. and Paro, R. 1999. Epigenetic inheritance of active chromatin after removal of the main transactivator. *Science* **286:** 955–958.

Cross, H.A. and Enver, T. 1997. The lineage commitment of haemopoietic progenitor cells. *Curr. Opin. Genet. Dev.* **7:** 609–613.

Di Croce, L., Koop, R., Venditti, P., Westphal, H.M., Nightingale, K.P., Corona, D.F.V., Becker, P.B., and Beato, M. 1999. Two step synergism between the progesterone receptor and the DNA-binding domain of nuclear factor 1 on MMTV minichromosomes. *Mol. Cell* **4:** 45–54.

Dölle, A. and Strätling, W.H. 1990. Genomic footprinting of proteins interacting with the chicken lysozyme promoter. *Gene* **95:** 187–193.

Fritton, H.P., Igo-Kemenes, T., Nowock, J., Strech-Jurk, U., Theisen, M., and Sippel, A.E. 1984. Alternative sets of DNase I-hypersensitive sites characterize the various functional states of the chicken lysozyme gene. *Nature* **311:** 163–165.

——— 1987. DNase I-hypersensitive sites in the chromatin structure of the lysozyme gene in steroid hormone target and non-target cells. *Biol. Chem. Hoppe-Seyler* **368:** 111–119.

Gale, J.M., Nissen, K.A., and Smerdon, M.J. 1987. UV-induced formation of pyrimidine dimers in nucleosomal core DNA is strongly modulated with a periodicity of 10.3 bases. *Proc. Natl. Acad. Sci.* **84:** 6644–6648.

Goethe, R. and Phi van, L. 1994. The far upstream chicken lysozyme enhancer at –6.1 kilobase, by interacting with NF-M, mediates lipopolysaccharide-induced expression of the chicken lysozyme gene in chicken myelomonocytic cells *J. Biol. Chem.* **269:** 31302–31309.

Graf, T., McNagny, K., Brady, G., and Frampton, J. 1992. Chicken "erythroid" cells transformed by the gag-myb-ets-encoding E26 leukemia virus are multipotent. *Cell* **70:** 201–213.

Grewal, T., Theisen, M., Borgmeyer, U., Grussenmeyer, T., Rupp, R.A.W., Stief, A., Qian, F., Hecht, A., and Sippel, A.E. 1992. The –6.1-kilobase chicken lysozyme enhancer is a multifactorial complex containing several cell-type-specific elements. *Mol. Cell Biol.* **12:** 2339–2350.

Gross, D.S. and Garrard, W.T. 1988. Nuclease hypersensitive sites in chromatin. *Annu. Rev. Biochem.* **57:** 159–197.

Gualdi, R., Bossard, P., Zheng, M., Hamada, Y., Coleman, J.R., and Zaret, K.S. 1996. Hepatic specification of the gut endoderm in vitro: Cell signaling and transcriptional control. *Genes & Dev.* **10:** 1670–1682.

Hershkowitz, M. and Riggs, A.D. 1997. Ligation-mediated PCR for chromatin-structure analysis of interface and metaphase chromatin. *Methods* **11:** 253–263.

Huber, M.C., Bosch, F., Sippel, A.E., and Bonifer, C. 1994. Chromosomal position effects in chicken lysozyme gene transgenic mice are correlated with suppression of DNaseI hypersensitive site formation. *Nucleic Acids Res.* **22:** 4195–4201.

Huber, M.C., Graf, T., Sippel, A.E., and Bonifer, C. 1995. Dynamic changes in the chromatin of the chicken lysozyme gene domain during differentiation of multipotent progenitors to macrophages. *DNA Cell Biol.* **14:** 397–402.

Huber, M.C., Jägle, U., Krüger, C., and Bonifer, C. 1997. The developmental activation of the chicken lysozyme locus in transgenic mice requires the interaction of a subset of enhancer elements with the promoter. *Nucleic Acids Res.* **25:** 2992–3000.

Huber, M.C., Krüger, G., and Bonifer, C. 1996. Genomic position effects lead to an inefficient reorganization of nucleosomes in the 5′-regulatory region of the chicken lysozyme locus in transgenic mice. *Nucleic Acids Res.* **24:** 1443–1453.

Hu, M., Krause, D., Greaves, M., Sharkis, S., Dexter, M., Heyworth, C., and Enver, T. 1997. Multilineage gene expression precedes commitment in the hemopoietic system. *Genes & Dev.* **11:** 774–785.

Ikuta, T., Kan, Y.W., Swerdlow, P.S., Faller, D.V., and Perrine, S.P. 1998. Alterations in protein–DNA interactions in the

γ-globin gene promoter in response to butyrate therapy. *Blood* **92:** 2924–2933.

Jägle, U., Müller, A.M., Kohler, H., and Bonifer, C. 1997. Role of positive and negative cis-regulatory elements regions in the regulation of transcriptional activation of the lysozyme locus in developing macrophages of transgenic mice. *J. Biol. Chem.* **272:** 5871–5879.

Jiménez, G., Griffith, S.D., Ford, A.M., Greaves, M.F., and Enver, T. 1992. Activation of β-globin locus control region precedes commitment to the erythroid lineage. *Proc. Natl. Acad. Sci.* **89:** 10618–10622.

Katz, S., Kowenz-Leutz, E., Müller, C., Meese, K., Ness, S.A., and Leutz, A. 1993. The NF-M transcription factor is related to C/EBPβ and plays a role in signal transduction, differentiation and leukemogenesis of avain myelomonocytic cells. *EMBO J.* **12:** 1321–1332.

Kikyo, N. and Wolffe, A.P. 2000. Reprogramming nuclei: Insights from cloning, nuclear transfer and heterokaryons. *J. Cell Sci.* **113:** 11–20.

Komura, J. and Riggs, A.D. 1998. Terminal deoxynucleotidyl transferase-dependent PCR, a new, more sensitive approach to genomic footprinting and adduct detection. *Nucleic Acids Res.* **26:** 1807–1811.

Kouzarides, A. 2000. Acetylation: A regulatory modification to rival phosphorylation? *EMBO J.* **19:** 1176–1179.

Krüger, G., Huber, M., and Bonifer, C. 1999. The –3.9 kb DHS of the chicken lysozyme locus harbors an enhancer with unusual chromatin reorganizing activity. *Gene* **236:** 63–77.

Kulessa, H., Frampton, J., and Graf, T. 1995. GATA-1 reprograms avian myelomonocytic cell lines into eosinophils, thromboblasts and erythroblasts. *Genes & Dev.* **9:** 1250–1262.

Li, Q., Imhof, A., Collingwood, T.N., Urnov, F.D., and Wolffe, A.P. 1999. p300 stimulates transcription instigated by ligand-bound thyroid hormone receptor at a step subsequent to chromatin disruption. *EMBO J.* **18:** 5634–5652.

Maxam, A.M. and Gilbert, W. 1980. Sequencing end-labelled DNA with base specific chemical cleavages. *Methods Enzymol.* **65:** 499–560.

Metz, T. and Graf, T. 1991. v-myb and v-ets transform chicken erythroid cells and cooperate both in trans and in cis to induce distinct differentiation phenotypes. *Genes & Dev.* **5:** 369–380.

Norton, V.G., Imai, B.S., Yau, P., and Bradbury, E.M. 1989. Histone acetylation reduces nucleosome core particle linking number change. *Cell* **57:** 449–457.

O'Neill, L.P. and Turner, B.M. 1999. Histone H4 acetylation distinguishes coding regions of the human genome from heterochromatin in a differentiation-dependent but transcription-independent manner. *EMBO J.* **14:** 3946–3957.

Pfeifer, G.P., Drouin, R., Riggs, A.D., and Holmquist, G.P. 1992. Binding of transcription factors generates hot spots for UV photoproducts in vivo. *Mol. Cell Biol.* **12:** 1798–1804.

Pfeifer, G.P., Chen, H.-H., Komura, J., and Riggs, A.D. 1999. Chromatin structure analysis by ligation-mediated and terminal-transferase mediated polymerase chain reaction. *Methods Enzymol.* **304:** 548–571.

Phi van, L. 1996. Transcriptional activation of the chicken lysozyme gene by NF-κ Bp65 (RelA) and c-Rel, but not by NF-κ Bp50. *Biochem. J.* **313:** 39–44.

Pina, B., Brüggemeier, U., and Beato, M. 1990. Nucleosome positioning modulates accessibility of regulatory proteins to the mouse mammary tumor virus promoter. *Cell* **60:** 719–731.

Roque, M.C., Smith, P.A., and Blasquez, V.C. 1996. A developmentally modulated chromatin structure at the mouse immunoglobulin κ 3′ enhancer. *Mol. Cell Biol.* **16:** 3138–3155.

Rundlett, S.E., Carmen, A.A., Suka, N., Turner, B.M., and Grunstein, M. 1998. Transcriptional repression by UME6 involves deacetylation of lysine 5 of histone H4 by RPD3. *Nature* **392:** 831–835.

Shaffer, A.L., Peng, A., and Schlissel, M.S. 1997. In vivo occupancy of the κ light chain enhancers in primary pro- and pre-B cells: A model for κ locus activation. *Immunity* **6:** 131–143.

Sippel, A.E., Borgmeyer, U., Püschel, A.W., Rupp, R.A.W., Stief, A., Strech-Jurk, U., and Theisen, M. 1987. Multiple nonhistone protein–DNA complexes in chromatin regulate the cell- and stage-specific activity of an eucaryotic gene. In *Results and problems in cell differentiation* (ed. W. Hennig), pp. 255–269. Springer, Berlin.

Sippel, A.E., Stief, A., Hecht, A., Müller, A., Theisen, A., Borgmeyer, U., Rupp, R.A.W., Grewal, T., and Grussenmeyer, T. 1989. The structural and functional domain organization of the chicken lysozyme gene locus. In *Nucleic acids and molecular biology* (ed. F. Eckstein and D.M.J. Lilley), pp. 133–147. Springer, Berlin.

Strahl, B.D. and Allis C.D. 2000. The language of covalent histone modifications. *Nature* **403:** 41–45.

Straka, C. and Hörz, W. 1991. A functional role for nucleosomes in the repression of a yeast promoter. *EMBO J.* **14:** 1727–1736.

Struhl, K. 1998. Histone acetylation and transcriptional regulatory mechanisms. *Genes & Dev.* **12:** 599–606.

Tenen, D.G., Hromas, R., Licht, J.D., and Zhang, D.E. 1997. Transcription factors, normal myeloid development, and leukemia. *Blood* **90:** 489–519.

Theisen, M., Stief, A., and Sippel, A.E. 1986. The lysozyme enhancer: Cell-specific activation of the chicken lysozyme gene by a far-upstream element. *EMBO J.* **5:** 719–724.

van der Vlag, J. and Otte, A.P. 1999. Transcriptional repression mediated by the human polycomb-group protein EED involves histone deacetylation. *Nat. Genet.* **23:** 474–477.

Yoo, J., Herman, L.E., Li, C., Krantz, B.S., and Tuan, D. 1996. Dynamic changes in the locus control region of erythroid progenitor cells demonstrated by polymerase chain reaction. *Blood* **87:** 2558–2567.

Zhang, W., Bone, J.R., Edmondson, D.G., Turner, B.M., and Roth, S.Y. 1998. Essential and redundant functions of histone acetylation revealed by mutation of target lysine and loss of the Gcn5p acetyltransferase. *EMBO J.* **17:** 3155–3167.